Project Report

Srinivasan Kidambi
Dept. of Electrical Engineering
Indian Institute of Technology, Madras
Chennai, India
ee21b139@smail.iitm.ac.in

Ayushman Agarwal
Dept. of Electrical Engineering
Indian Institute of Technology, Madras
Chennai, India
ee21b027@smail.iitm.ac.in

***Abstract*—In this report we seek to explain our work on phaseless direction of arrival estimation for 6G communication. We present the existing methods and subsequently our improvements to said methods to better the performance for high frequency carrier waves. Further, we apply this algorithm with two phased array antennae working in conjunction to further improve the resolution of the estimated angle of arrival.**

***Index Terms*—IRS, DoA estimation, Antenna Arrays, 6G, Optimization**

I. Introduction

In the field of communication, higher carrier frequencies, while increasing the data bandwidth, have some significant drawbacks. Chief among these is the inability to diffract off of solid corners, a core expectation for signal coverage. As a remedy to this issue, the use **intelligent reflective surfaces** or IRS for short is a solution being actively explored. The IRS allows for directed reflection of an incoming signal to the user, eliminating the reliance on passive diffraction.

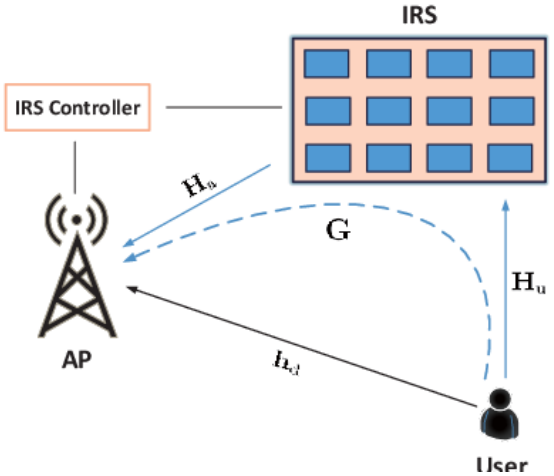

Fig. 1. Use of an IRS for communication

However, for this endeavour to succeed, one crucial requirement is that the IRS be able to locate the user. This is possible by using direction of arrival estimation algorithms which can latch onto a signal from the user's communication device and locate the user in real time. The development of such algorithms is an active area of research, one in which we base our UGRC project as well.

While most DoA algorithms currently use the entire received signal to estimate the angle of arrival, we aim to develop a reliable algorithm to complete the task using just the measured power of the incoming signal, i.e. without utilizing phase data. This helps cut down costs and also eliminates the effect of unreliable phase measurements. To achieve this, we fall back onto phased array antenna hardware, which allows for efficient directive beamforming.

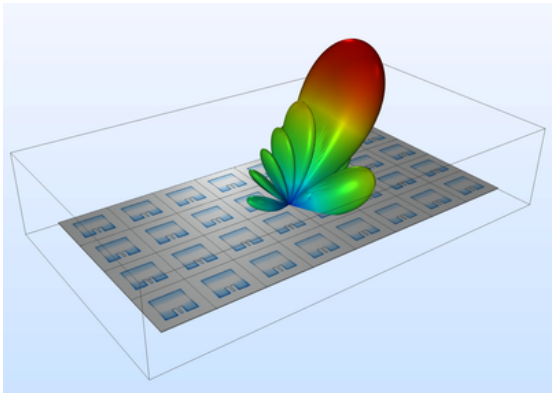

Fig. 2. Phased array antennae allow for effective beamforming

II. Literature Review

In order to gain a deeper understanding of our problem statement and the current ongoing research in the area, we went through relevant papers and existing algorithms. We tried to understand each aspect in depth and did our own implementations wherever required. In this section, we describe some of the papers and algorithms, the concepts involved and our key takeaways.

A. MUSIC: Multiple Signal Classification

This method proposes a Direction of Arrival (DoA) estimation technique for L unlocated signals using the received signal information, i.e. both magnitude and phase information. This is achieved by isolating the bases for the signal and noise subspaces and searching for peaks in the pseudo spectrum.

Signal Model

The sampled signal is modelled as :

$$\mathbf{x}_n = [\mathbf{a}(\theta_0)\mathbf{a}(\theta_1)...\mathbf{a}(\theta_{L-1})]\mathbf{s}_n + \mathbf{n}_n = \mathbf{A}\mathbf{s}_n + \mathbf{n}_n \quad (1)$$

where,

- M is the number of sensors
- L is the number of unlocated signals
- $x_n \in \mathbb{C}^M$ is the sampled signal vector
- $A \in \mathbb{C}^{M \times L}$ is the array matrix
- $s_n \in \mathbb{C}^L$ is the received signal vector
- $n_n \in \mathbb{C}^M$ contains the AWGN noise elements n_k[n]

Eigenstructure of the Spatial Covariance Matrix
The spatial covariance matrix of the sampled signals is found:

$$\mathbf{R} = \mathbb{E}[\mathbf{x}_n \mathbf{x}_n^H] = \mathbf{A}\mathbf{R}_{ss}\mathbf{A}^H + \sigma^2 \mathbf{I}_{MxM}$$

From the above definition, we can see that R is Hermitian. Now, we perform an eigen decomposition of the obtained covariance matrix to get the eigenvalues and their corresponding eigenvectors. We arrange the obtained M eigenvalues in descending order and choose the first L eigenvalues, i.e. the L largest eigenvalues and their corresponding eigenvectors.

$$\lambda_1 \geq \lambda_2 \geq ... \geq \lambda_M > 0, \tag{2}$$

The L largest eigenvalues correspond to the L signal sources and their eigenvectors span a subspace called the signal subspace. The remaining M - L eigenvalues correspond to noise and their corresponding eigenvectors span a subspace called the noise subspace.

By spectral theorem for hermitian matrices, the noise and signal subspaces are orthogonal to each other. The steering vectors $a(\theta_l)$, i.e. the columns of A, lie in the signal subspace. Therefore, the steering vectors are orthogonal to the noise subspace.

Because the true sensor covariance matrix is not known, MUSIC estimates the sensor covariance matrix, R, from the sample sensor covariance matrix. The sample sensor covariance matrix is an average of multiple snapshots of the sensor data as given below:

$$\hat{\mathbf{R}} = \frac{1}{S} \sum_{n=0}^{S-1} \mathbf{x}_n \mathbf{x}_n^H$$

Psuedo-Spectrum
The final step involves defining a psuedo-spectrum as:

$$\mathbf{P}_{MUSIC}(\theta) = \frac{1}{\mathbf{a}^H(\theta)\mathbf{Q}_n\mathbf{Q}_n^H\mathbf{a}(\theta)}$$

where, Q_n is a Mx$(M-L)$ matrix whose columns correspond to the noise eigenvectors.

If $a(\theta)$ is a steering vectors corresponding to one of the incoming signals, then the denominator becomes 0 (due to the aforementioned orthogonality of the signal and noise subspaces), and we get a peak in the pseudo spectrum. **Detecting these peaks gives us the required DoAs**. Since we have estimated $\hat{\mathbf{R}}$ using samples, the denominator won't be exactly 0 but will instead be close to 0 due to the error in Q_n.

Key Takeaways

Our key takeaways from this approach are as follows:

- We understood an existing approach for signal DoA estimation and the requirement of phase information in such methods.
- The difference between one shot DoA estimation as in this algorithm and the requirement for beamforming in subsequent phaseless DoA estimation methods.

B. Fine-grained azimuthal Direction of Arrival estimation using received signal strengths (Maddio et al. , 2017)

This paper proposes a Direction of Arrival (DoA) estimation technique, enabled by a patch antenna capable of producing four reconfigurable beams at the operative frequency of 2.45Ghz.

This is achieved by correlating the real time received signal strength data (No phase data required) with the expected antenna beams.

The comparison is implemented with a least square technique. Experimental validations demonstrate the DoA estimation capability, with a mean error $\leq$ 2.3° with a variance of 1.9° within a domain of 90°

The Antenna
The antenna used in the positioning system is a circular polarized bi modal patch antenna.

It consists of two concentric annular patches printed in common FR4 substrate. Each of these elements operates in a different mode (hence, bimodal). Also, there are 8 parasitic elements around the external patch.

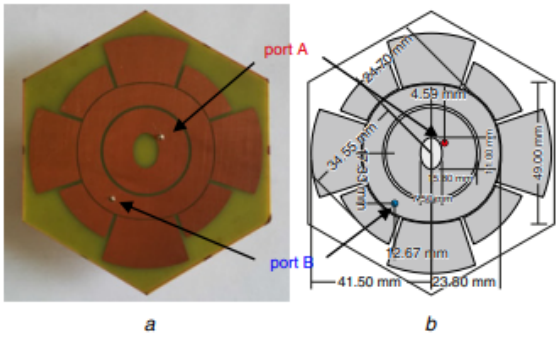

Fig. 3. Circularly polarized bi modal antenna

- The inner patch operates in TM_{11} mode and radiates a directional beam with a maximum towards 0°
- The outer patch operates in TM_{21} mode and radiates a conical beam pattern with its maximum in the region around 45°
- 8 parasitic crown shaped elements are arranged around the external disk in alternating manner to enhance the gain of the external patch.

Beamformer Architecture

The components present are:

- 2 half power splitters
- A hybrid ring coupler

Using a combination of these components, we are able to generate four possible beam patterns.

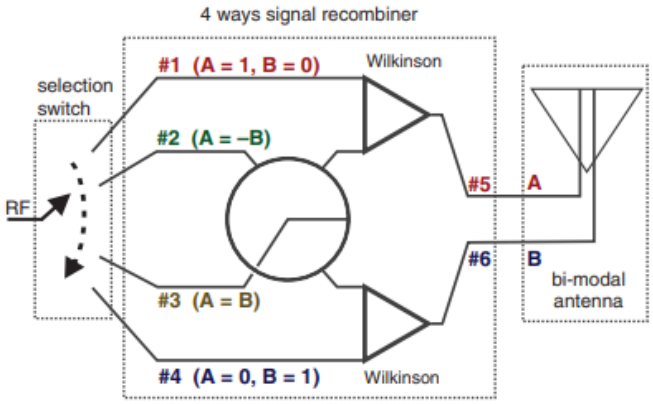

Fig. 4. Beamformer Architecture

Here is how we obtain each of the 4 beams:

- Selecting input port $\#1$ gives rise to a directive beam as port $\#5$ is connected to antenna input A, resulting in the isolation of port $\#6$. We identify this beam as beam $\#1$.
- When input $\#2$ is selected, ports $\#5$ and $\#6$ are excited with the same power but in anti-phase. As a consequence, the antenna ports A and B are simultaneously excited, and a tilted beam identified with $\#2$ is obtained, pointing approximately towards $30°$ in the horizontal plane.
- Similarly, selecting the input port $\#3$ excites the in-phase combination of $\#5$ and $\#6$, and a beam pointing towards $-30°$ is generated, serving as beam $\#3$.
- The signal entering into port $\#4$ is totally routed towards port $\#6$, thus resulting in the isolation of port $\#5$, which is the opposite of the directive beam case. The antenna input B is therefore exclusively excited, generating the conic beam labelled as $\#4$.

The selection of one of the four paths is activated with a switch connected to the four inputs of the beam former as shown in the figure.

System Setup

The configuration of the system for Direction of Arrival estimation has been depicted in figure 3.

The positioning system consists of the source node emitting the signal and the receiver consisting of the bi-modal patch antenna and the beamforming architecture.

We employ a beam switching communication mechanism to estimate the direction of arrival, i.e. we sequentially switch through the various beams in our beamset and measure the RSSI for each such configuration.

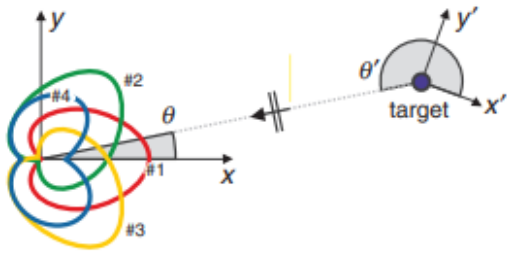

Fig. 5. System Setup

Azimuthal DoA estimation Approach

In the proposed approach, the direction of arrival is estimated using a comparison between the expected received relative signal magnitude (given by the difference in beam gains), and the real measured RSSI values for the various beam patterns.

When the unknown located target is in broadcast mode, the sequence of messages are received by the anchor sequentially throughout the beam set, and stored as a vector of RSSI readings.

The Line of Sight contribution is assumed to be the dominant component.

Let the source of the signal be present at an angle θ with respect to our DoA estimator. The received RSSI can be modelled using the following equation, popularly known as the Friis Relation:

$$RSSI_n = G_n(\theta) + L(D) + G_T(\theta^{'}) + P_T + w_n \quad (3)$$

- $G_n(\theta)$ is the gain of the nth beam.
- $G_T(\theta^{'})$ is the gain of the source.
- $L(D)$ is the free space loss due to the distance D.
- P_T is the transmitted power.
- w_n is the noise term.

This relation forms the crux behind the working of the proposed approach. The idea is to measure the RSSI for the directive and conical beams and compare their difference with the difference in gains of the two beams. For the correct DoA estimate, the two differences will have the same value(following from the Friis Relation). This approach allows us to estimate the DoA without any prior knowledge of the distance D or the source gain G_T.

Since the beams are symmetrical, this first comparison results in two possible estimates for the azimuthal angle of arrival. This is where the remaining two beams play a role. Since these beams are asymmetrical, we use their difference to estimate if the angle of arrival lies in the left quadrant or right quadrant. The same can be observed from the differential gain plots.

We can capture these above ideas mathematically using a suitable least square based objective function, resulting in an algorithm to compute the DoA estimate.

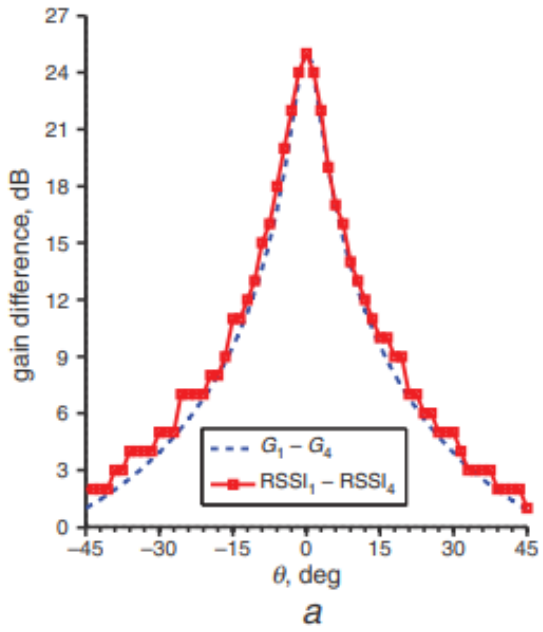

Fig. 6. Comparison of measured RSSI and differential gain for 1st pair of beams

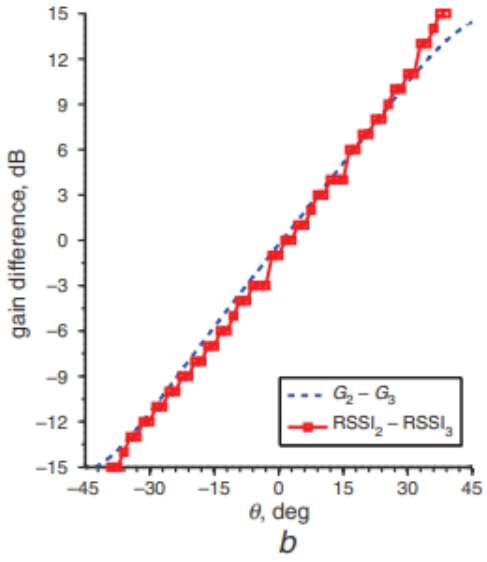

Fig. 7. Comparison of measured RSSI and differential gain for 2nd pair of beams

The objective/cost function is defined as below:

$$c(\theta) = \sqrt{(RSSI_1 - RSSI_4)^2 - (G_1(\theta) - G_4(\theta))^2} \quad (4)$$

We scan over a range of angles and our estimate is the angle which best fits the defined cost function.

As explained previously, the resulting estimate from the above cost function has a sign ambiguity which is resolved using the remaining pair of asymmetrical beams by observing the sign of $RSSI_1 - RSSI_3$

$$\hat{\theta} = argmin(c(\theta)) \cdot sign(RSSI_2 - RSSI_3) \quad (5)$$

Results

Below we present the results for this approach as published by the authors.

Distance	1.75 m	2.00 m	2.25 m	2.50 m	2.75 m	All
Mean	2.6°	3.2°	2.1°	1.9°	1.5°	2.3°
Std	2.4°	2.0°	1.5°	1.9°	1.0°	1.9°
90%	6.5°	5.5°	4.0°	3.5°	2.5°	5.0°

Fig. 8. DoA estimation for various scenarios

Key Takeaways

Our key takeaways from this approach are as follows:

- We were introduced to the idea of utilizing a set of beams instead of relying on just one to estimate the DoA.
- The use of the difference in beam gains and RSSIs to get rid of the unknown terms in the Friis relation was one of our key takeaways from this approach.
- The use of asymmetrical beams to resolve the sign ambiguity was another crucial idea which helped us in our own approach.

III. Developed Algorithms

We now describe the sequence of developments to the algorithm developed over the course of this project.

A. First Version

Brief Introduction to the Approach

In our initial approach, we tried to implement a set of beams using Phased Array Antennas to estimate the Direction of Arrival using just the RSSI (i.e. Received Signal Strength) data. We implemented two symmetrical beams using a Uniform Linear Array(ULA), and another asymmetrical beam using a Uniform Circular Array(UCA) to resolve the sign ambiguity, i.e whether the signal is arriving from the left quadrant or the right quadrant.

Initially, we were working with just Uniform Linear Arrays, but on further analysis of the array factor, we realized that a ULA can only give symmetrical beams irrespective of how the array element specific phases (i.e. weights) are tuned, which made us explore alternate options like a UCA.

Antenna Arrays Used

Below we have provided some basic specifications for the antenna arrays used, i.e. Uniform Linear Array and Uniform Circular Array.

Uniform Linear Array Specifications

- Number of Elements : 2
- Element Spacing : $\lambda/2$

Uniform Circular Array Specifications

- Number of Elements : 12
- Radius : $\lambda/3$

Since there are a total of 12 elements in the circular array, the angular separation between any two elements is 30°

Incident Signal

The incident signal can be given by

$$x = Ae^{j2\pi f_c} \tag{6}$$

, where

- A : Amplitude of incoming signal, which we have taken as 1 in our analysis
- f_c : Carrier frequency, which we have taken as 1GHz.

Received Signal at the Uniform Linear Array

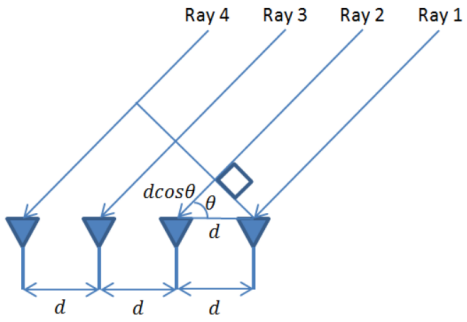

Fig. 9. ULA Diagram showing incoming signal rays

The received signal by the ith ULA element at the nth time instant can be given by

$$y_{n,i} = x * e^{-j2\pi f_c(i-1)\frac{d}{c}sin(\theta)} e^{-j2\pi f_c \frac{n}{f_{sampling}}} \tag{7}$$

Here,

- θ is the angle of incidence or the DOA angle being estimated. (θ is measured from the horizontal)
- f_c is the carrier frequency
- d is the element spacing of the array
- $f_{sampling}$ is the sampling frequency

The first exponential accounts for the phase delay introduced due to the position of the ith element, as can be seen from the diagram above.

The second exponential accounts for the phase delay due to the chosen sampling time instant.

Received Signal at the Uniform Circular Array

The received signal by the ith UCA element at the nth time instant can be given by

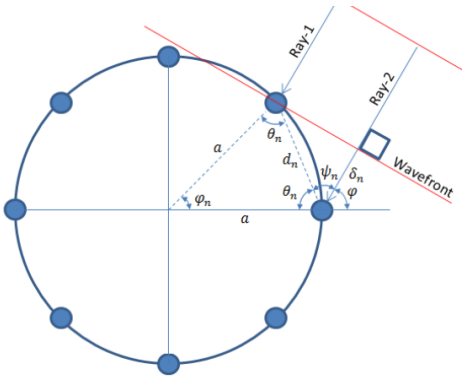

Fig. 10. UCA Diagram showing incoming signal rays

$$y_{n,i} = x * e^{-j*2\pi\frac{r}{\lambda_c}(cos(\theta-\theta_i)-cos(\theta))} e^{-j2\pi f_c \frac{n}{f_{sampling}}} \tag{8}$$

Here,

- θ is the angle of incidence
- r is the array radius
- λ_c is the carrier wavelength
- θ_i is the angular position of the element of the array

Just like before, the first exponential accounts for the phase delay due to the spatial position of the UCA element, and the second exponential accounts for the phase delay due to the chosen sampling time instant.

ULA Beamforming

The ULA beam pattern is given by the ULA array factor whose expression is as follows:

$$AF(\theta) = \sum_{i=1}^{N} a_i e^{-j*2\pi*(i-1)*\frac{d}{\lambda_c}*sin(\theta)} \tag{9}$$

where,

- θ is the angle of directivity of the beam
- d is the element spacing
- λ_c is the carrier wavelength
- N is the number of elements in the array
- a_i is the beamforming weight at the element of the array

We specify two different directive angles to the ULA, and obtain corresponding weights which can then be used to produce the desired beam. For our analysis, after a lot of experimentation, we arrived at directive angles 55° and 40° for the two symmetric ULA beams.

The expressions for weights are as follows:

$$a_i = e^{j2\pi(i-1)\frac{d}{\lambda_c}sin(\theta)} \tag{10}$$

where, θ is the specified angle of directivity.

The beam patterns for the two symmetric ULA beams (after conversion to decibels) we have used have been shown in the figures that follow:

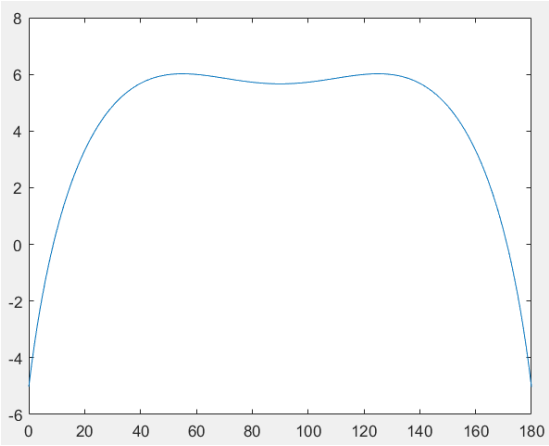

Fig. 11. Beam 1

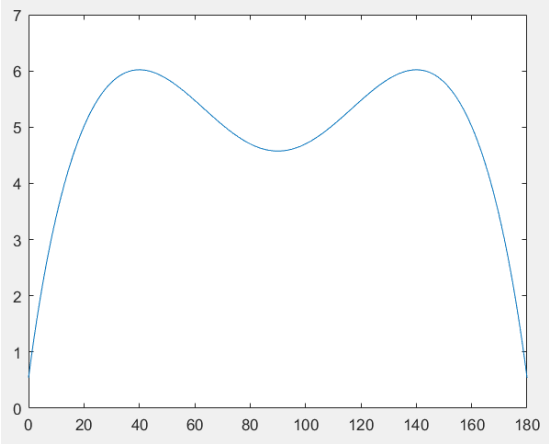

Fig. 12. Beam 2

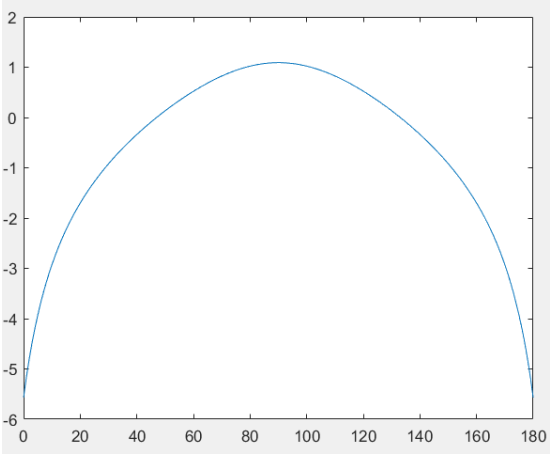

Fig. 13. Differential Gain of Beam 1 and Beam 2

UCA Beamforming

The UCA beam patterns are also given by their array factor expression as shown below:

$$AF(\theta) = \sum_{i=1}^{N} a_i e^{-j*2pi*\frac{r}{\lambda_c}*(cos(\theta-\theta_i)-cos(\theta))} \quad (11)$$

Here,

- θ is the specified angle of directivity for the beam
- a_i is the beamforming weight for the ith element
- N is the total number of array elements

For our purposes, we have used binary weight values, i.e. 1s or 0s for the UCA. We have used 1s for the elements in the first quadrant (i.e. these elements are simply ON), whereas we have used 0 weight values for the rest of the elements(i.e. they are turned OFF or need not even be present). This choice of weights helps us obtain a desirable asymmetric beam which can help us resolve the sign ambiguity.

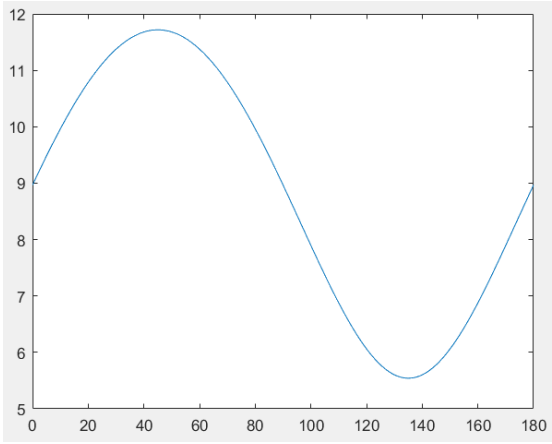

Fig. 14. Beam 3

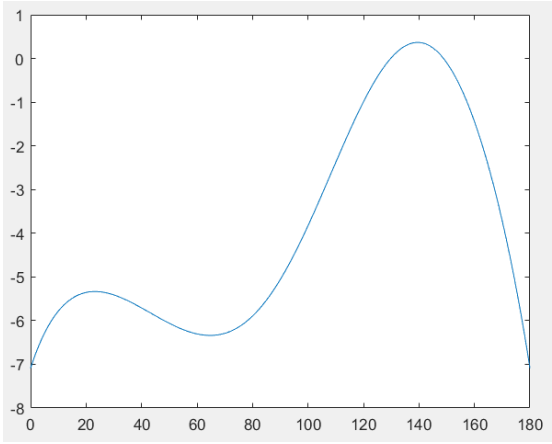

Fig. 15. Differential Gain of Beam 1 and Beam 3

RSSI Calculation

For any given incident signal, we calculate the RSSI by calculating the magnitude squared of the detected signal after it has been multplied element-wise by the weights applied at

each array element. We then take a time average over the sampled time instants to give us single RSSI values.

DoA Estimation

The DoA estimation algorithm is as follows:

- We find the differential gain between Beam 1 and Beam 2, i.e. the two symmetrical beams and compare it with difference of the detected RSSIs for the two beams. The angles which for which these two values are the closest are considered to be potential solutions for the estimation. Due to the symmetric nature of these beams, we get two values.
- This ambiguity is then resolved by using the asymmetric beam generated by the UCA, i.e. Beam 3. We again compute a differential gain between a symmetrical and an asymmetrical beam and compare it with the difference of the corresponding detected RSSIs. The angle among the two for which these values are closer is the final estimate returned by the algorithm.

The cost function can be expressed as follows:

$$c(\theta) = \sqrt{(RSSI_1 - RSSI_2)^2 - (G_1(\theta) - G_2(\theta))^2} \quad (12)$$

Results

We ran the algorithm described for various values of total number of iterations. The obtained error plots have been shown below:

Number of Iterations = 10

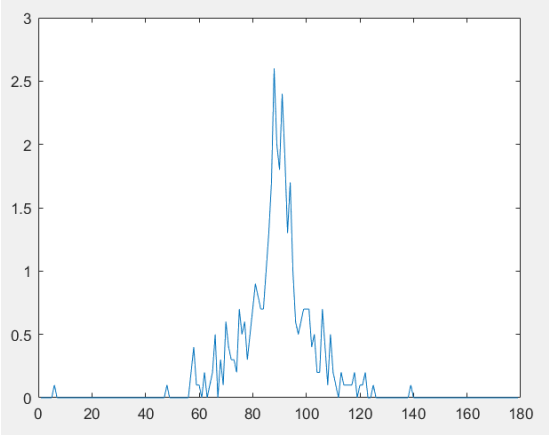

Fig. 16. Mean Error vs angle of incidence for n = 10

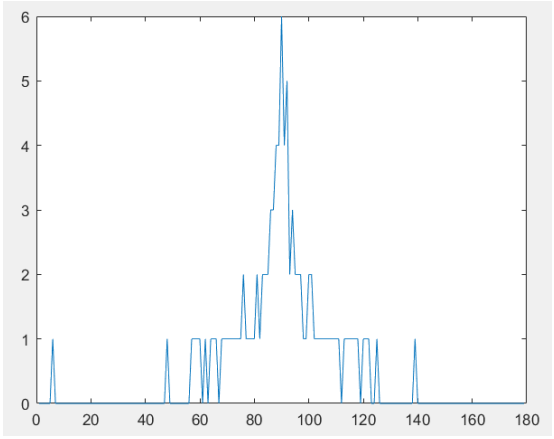

Fig. 17. Max Error vs angle of incidence for n = 10

Number of Iterations = 20

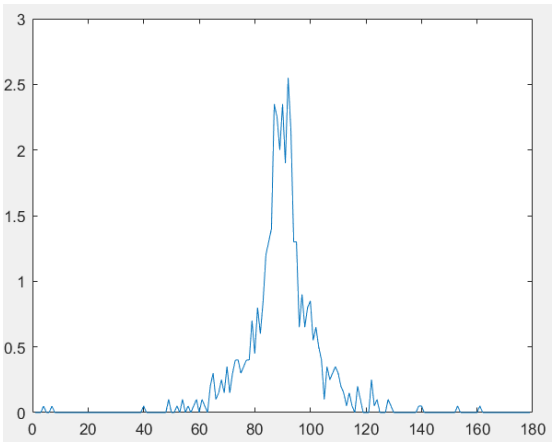

Fig. 18. Mean Error vs angle of incidence for n = 20

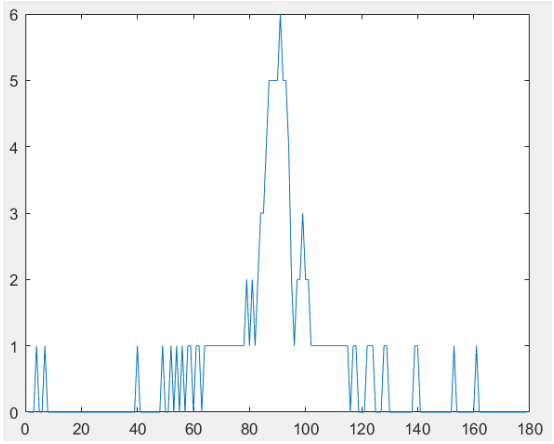

Fig. 19. Max Error vs angle of incidence for n = 20

Number of Iterations = 30

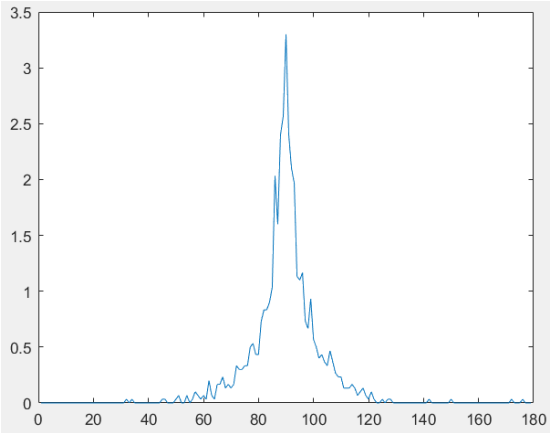

Fig. 20. Mean Error vs angle of incidence for n = 30

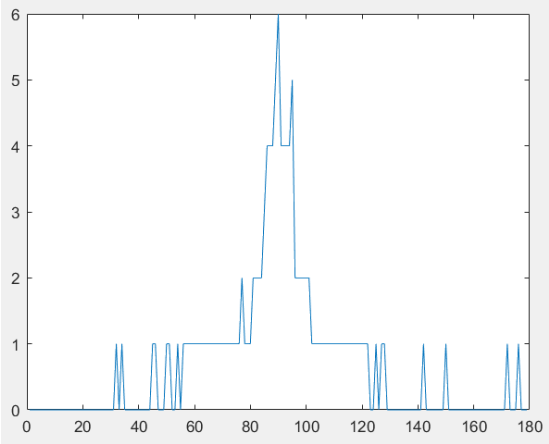

Fig. 21. Max Error vs angle of incidence for n = 30

The tabulated average errors obtained for various number of iterations for this approach are shown below:

Num Iterations	Avg Error
10	0.2285
20	0.2215
30	0.2214

B. Final Version

Antenna Arrays Used

Below we have provided some basic specifications for the antenna arrays used, i.e. Uniform Linear Array and Uniform Circular Array.

Uniform Linear Array Specifications

- Number of Elements : 2
- Element Spacing : $\lambda/2$

Uniform Circular Array Specifications

- Number of Elements : 12
- Radius : $\lambda/3$

Since there are a total of 12 elements in the circular array, the angular separation between any two elements is 30°

Drawbacks of the first approach

From the experimental results of the first approach we observed the following drawbacks with that attempt:

- The performance around the central angles is much worse than other incident angles.
- The sensitivity in the central region is quite low

These issues can be explained by analyzing the differential symmetric beam in figure 13. We observe that around the central angles, the slope of the differential gain beam is quite low. The flat nature of the beam results in the poor resolution.

Resolution in central region

In order to rectify the low slope problem in the differential gain beam, the algorithm was conditioned on the predicted angle:

- The initial approach was used without modification in the peripheral region.
- If the predicted angle was found to be in the low sensitivity central region, a different differential gain beam was used instead of the original ULA version. This beam is obtained from the UCA beam intially used and a new ULA beam whose weights are offset by a phase of $\pi/2$.

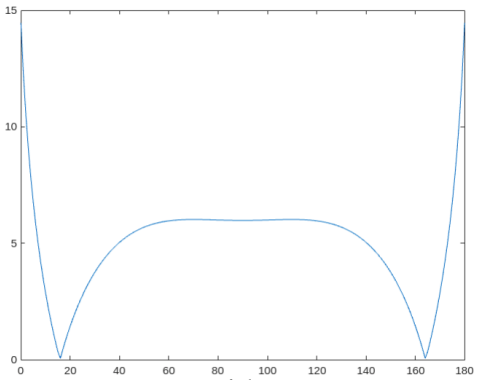

Fig. 22. Beam 4

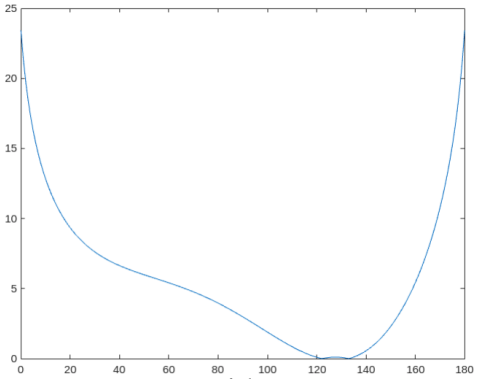

Fig. 23. Differential Gain of Beam 3 and Beam 4

Results

We ran the algorithm described for various values of total number of iterations. The obtained error plots have been shown below:

Number of Iterations = 10

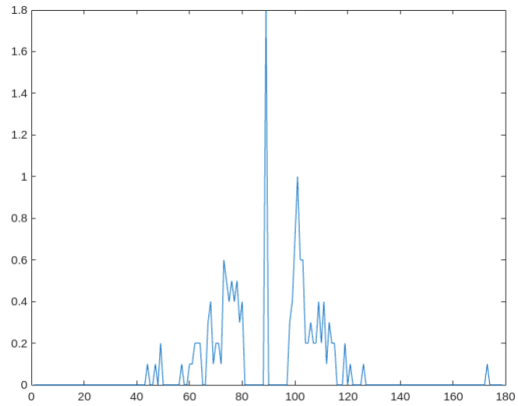

Fig. 24. Mean Error vs angle of incidence for n = 10

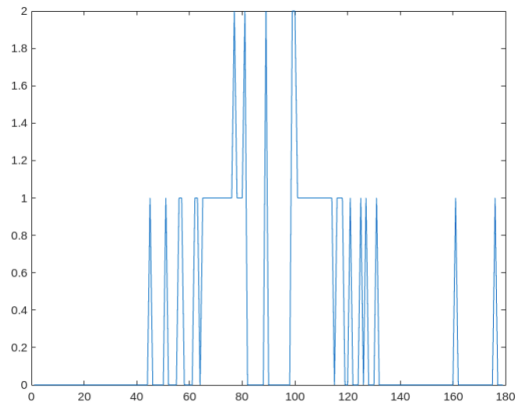

Fig. 25. Max Error vs angle of incidence for n = 10

Number of Iterations = 20

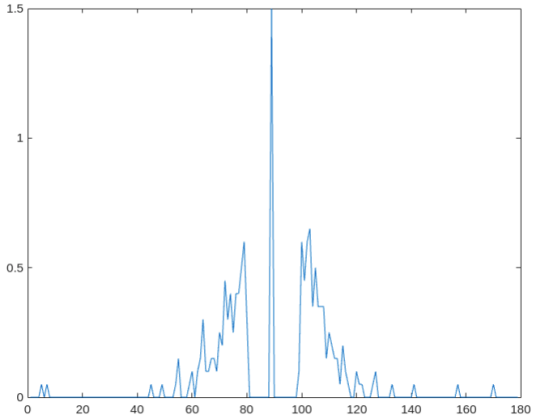

Fig. 26. Mean Error vs angle of incidence for n = 20

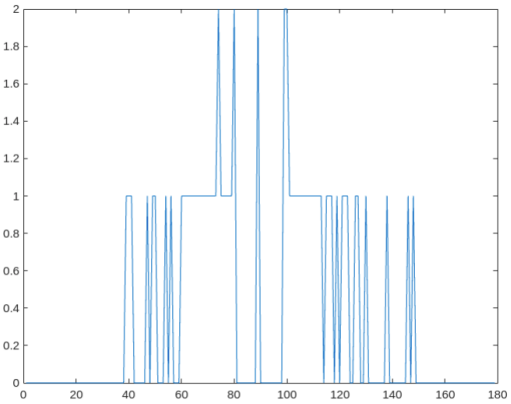

Fig. 27. Max Error vs angle of incidence for n = 20

Number of Iterations = 30

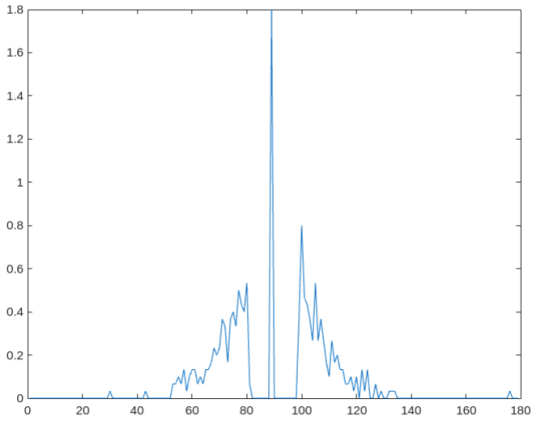

Fig. 28. Mean Error vs angle of incidence for n = 30

The tabulated average errors obtained for various number of iterations for this approach are shown below:

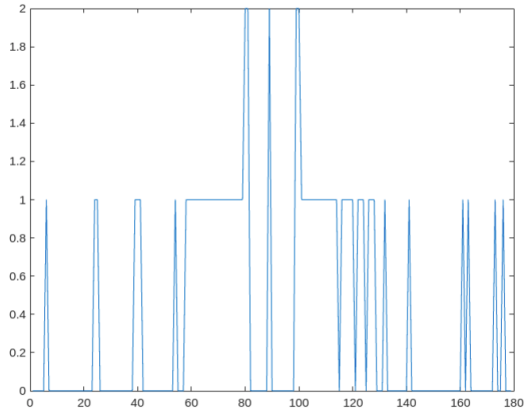

Fig. 29. Max Error vs angle of incidence for n = 30

Num Iterations	Avg Error
10	0.0788
20	0.0751
30	0.0724

Observations

We see from the results and plots that both the mean error and the max error have dropped significantly. Further, we observe that the error in the central region has reduced significantly due to the increased slope of the replacement differential beam.

Optimization of weights (work in progress)

In order to formalize the approach used to improve the resolution at this stage, we cast the solution as an optimization problem over the weights of the phased array antennae. The objective is defined as:

$$C = G_1(\theta) - G_2(\theta) = 20log(|AF_1(\theta, \mu_1)|) - 20log(|AF_2(\theta, \mu_2)|)$$

where, μ_i are the weights of the i^{th} array. We wish to maximize the slope of this function over a range of azimuths (say $\theta 1$ to $\theta 2$).

$$\mu_1, \mu_2 = argmax(\int_{\theta_1}^{\theta_2} |\frac{d(C)}{d\theta}| \, d\theta)$$

when carrying out this optimization the following should be kept in mind:

- The sign for the slope of a differential ULA beam would change around the central angle. Hence the integral breaks there as we only require a high magnitude of slope and the sign is irrelevant.
- For a differential beam involving the UCA however, we desire the slope to be positive or negative continuously. This is to ensure the viability of the beam as the asymmetric beam used to resolve to a single angle from two angles.
- The limits of the integral would be the low sensitivity region so as to get steeper slopes where it is required as opposed to considering the entire azimuth range which would invariably only ensure the sum of slopes being maximized over multiple angles where the slope is already high.

Future Work

To further this research, we seek to take the following steps in the future:

- Utilize the optimization framwork proposed before to improve the resolution. Also try to improve the framework if possible.
- Test the algorithm with hardware in real time to analyze the precision-delay tradeoff. While running multiple iterations of the algorithm can effectively curb the effect of noise as seen above, the delay also increases, which may render the approach unsuitable to real world communication use.
- Generalize the algorithm for elevation of incoming signals as well. Currently, the elevation is assumed to be 0 which need not always be true.
- Improve the algorithm to deal with multiple sources at once. One of the main advantages of the MUSIC algorithm was the ability to deal with multiple sources simultaneously. We seek to incorporate this functionality in our algorithm as well.

Acknowledgment

We would like to express our gratitude to our guide Professor Uday Khankhoje whose support and expertise was a pillar of our progress throughout this project. Through this opportunity, we were introduced to practical work in the field of communication which broadened our horizons and gaining much experience in research.

References

[1] S. Maddio, A. Cidronali, M. Passafiume, G. Collodi, and S. Maurri (2017) "Finegrained azimuthal direction of arrival estimation using received signal strengths," Electron. Lett., vol. 53, no. 10, pp. 687–689, 2017 Phaseless DoA May 14, 2024 21 / 21